

EFFECTS OF LOAD INTERRUPTION ON THE FATIGUE LIFE OF GFRP COMPOSITES

A.Vahid Movahedi-Rad, Thomas Keller, and Anastasios P. Vassilopoulos

Composite Construction Laboratory (CCLab), Ecole Polytechnique Fédérale de Lausanne, (EPFL),
Station 16, Bâtiment BP, CH-1015 Lausanne, Switzerland
Email: anastasios.vasilopoulos@epfl.ch, <http://cclab.epfl.ch>

Keywords: Loading pattern, Damage mechanism, Fatigue stiffness, Dissipated energy, Self-generated temperature, Damage retardation mechanism,

Abstract

The effect of cyclic loading interruption on the fatigue behavior of angle-ply (± 45)_{2S} glass/epoxy composite laminates was investigated by comparing the obtained results of continuous- and interrupted loading patterns. Continuous fatigue experiments were performed by applying a sinusoidal cyclic loading pattern with maximum cyclic stresses at six different stress levels. For interrupted fatigue experiments, the cyclic loading was interrupted for two hours at regular intervals, corresponding to 20% of the fatigue life under continuous loading at the same maximum cyclic stress level. It was observed that the distribution and the severity of the fatigue damage was a function of loading pattern and stress level. Damage was more uniform when interrupted fatigue loading was applied. This loading pattern decelerated damage growth and increased the specimen's capacity to accumulate damage. The specimens loaded under interrupted fatigue exhibited longer fatigue lives than those continuously loaded. This enhancement of fatigue was more pronounced at high stress levels.

1. Introduction

Damage accumulates in the volume of composite materials during fatigue loading and eventually leads to failure. Several damage mechanisms, including fiber breakage, matrix cracking, debonding, transverse-ply cracking, and delamination, are activated either independently or synergistically during fatigue loading; the predominance of one or another is strongly affected by both material variables and the sequence and duration of the damage events [1]. The presence of these damage mechanisms results in the degradation of the materials properties under service loading conditions. Usually, failure of unidirectional, cross-ply, and angle-ply laminates can be characterized by a three-stage damage progression process, starting with the damage formation in the matrix with multiple crack development, followed by the initiation of matrix cracks reaching the vicinity of the fibers and matrix/fiber debonding and delaminations, and ending with fiber breakage when damage accumulated during the previous stages becomes saturated [2].

Due to the presence of the viscoelastic polymer matrix in a variety of laminated composites, the time-dependent mechanical properties of the material are also affected during fatigue loading, [1]. The time-dependent material behavior can be studied by observing the creep, recovery, and stress relaxation behavior of the material.

Cyclic-dependent and time-dependent phenomena usually interact during fatigue loading, and the degree of interaction, but also the dominance of one over another, depends on the loading spectrum and the material, [3]. Although works exist about the effects of the creep-fatigue interaction on the fatigue life of composites, the literature review showed that the effect of load interruption on the fatigue behavior of composite materials has not been extensively studied. The publications relevant to this topic that are available to the authors of this work, e.g., [4-7], clearly indicate a life extension due

to the load interruptions, but contain no description of the fatigue damage development and distribution in the material, or the fatigue failure mechanisms that occur. The previous studies were based on very limited experimental programs, mainly investigating the interrupted fatigue behavior at only one stress level and without giving more information regarding the experimental conditions, monitoring of the specimen temperature evolution, etc. Furthermore, there is no rational discussion regarding the interaction of the mechanisms (damage growth, cyclic creep, recovery), the material's capacity to dissipate energy, and their influence on fatigue life.

The objective of this work is to investigate the effect of loading interruption on fatigue behavior of glass fiber reinforced polymer (GFRP) laminates. Constant amplitude fatigue experiments with load interruptions were performed on $\pm 45^\circ$ angle-ply composite laminates at six different stress levels, and the obtained experimental results were compared to relevant fatigue data from continuous constant amplitude fatigue experiments. The material behavior was continuously monitored via measurement of the cyclic stress-strain and the self-generated temperature increase during the experiments. The evolution of the fatigue damage and the developed failure modes were also recorded by monitoring the variation of the material's transparency during the cyclic loading and studying, post-mortem, the fracture surfaces.

2. Experimental procedure

Rectangular glass/epoxy $[\pm 45]_{2s}$ composite specimens with the average dimensions of $250 \times 25 \times 2.3$ mm³ (length \times width \times thickness) were prepared, according to ASTM D3039. Fatigue experiments were performed by applying two types of sinusoidal patterns of continuous and interrupted fatigue loading. Fig. 1 shows a schematic representation of the applied interrupted loading profile, comprising repetitive loading blocks of constant amplitude up to the specimen's failure.

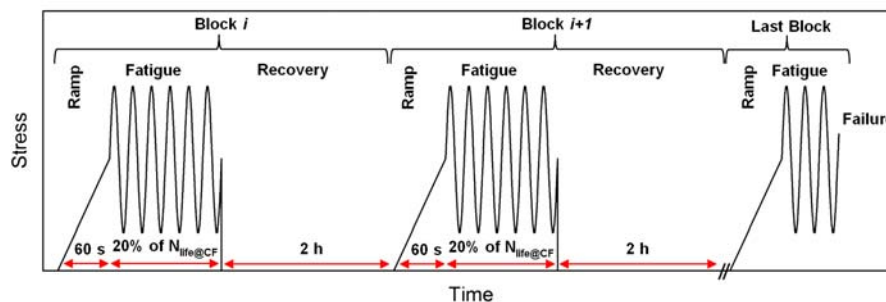


Figure 1. Schematic representation of the interrupted fatigue loading pattern.

For each experiment, the load was increased until the mean value was reached, after 60 seconds. Subsequently, the constant amplitude fatigue loading was applied for a predetermined number of cycles (20% of the average fatigue life estimated for the same stress levels under continuous loading), followed by a zero-load interval lasting for two hours. The duration of 20% of the fatigue life in each loading block was selected in order to obtain a certain number of interruptions in each fatigue experiment and a reasonable duration of the fatigue experiments. The transition from the mean fatigue loading to the zero-load intervals was achieved in one second. The cyclic loading was performed in the range of maximum stress levels of 47 MPa–68 MPa based on the ASTM D7791-17, similar to the stress levels selected for the continuous fatigue experiments performed in the previous work by the authors. The stress ratio, $R = \sigma_{\min} / \sigma_{\max}$, was kept constant to 0.1 in order to apply tensile cyclic loads to the specimens, while a constant loading rate of 30.5 kN/s was used for all experiments.

All experiments were performed in an environmental chamber regulated at a constant temperature of 20°C. Two fans were used to circulate the air inside the chamber and cool the specimens. The variation of the longitudinal strains was measured by a high-resolution video-extensometer with a frequency of acquisition of 160 images/s. An infrared (IR) thermal camera with an accuracy of 0.1°C was also employed during the fatigue experiments to record the evolution of the specimen's surface temperature. To detect the damage development in the translucent specimens at a macro-scale level,

photographs were taken at regular intervals (depending on the life expectancy) with a digital camera. After failure, the failure surfaces were examined using a digital handheld Dino-Lite microscope. More details of the experimental procedure can be found in [8,9].

3. Experimental results and discussion

3.1. Quasi-static behavior

Typical stress-strain curves of the examined laminates under the two different loading conditions are shown in Fig. 2. The specimens exhibited a rate-dependent, non-linear, stress-strain response. When the loading rate was increased, the value of yield stress (YS) and ultimate tensile stress (UTS) increased, although the strain to failure slightly decreased. The rate-dependent behavior was attributed to the viscoelastic behavior of the polymeric matrix.

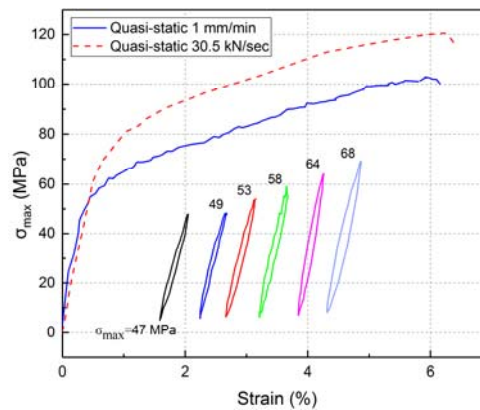


Figure 2. Quasi-static stress-strain curves and typical hysteresis loops at different stress levels.

3.2. Fatigue behavior

The fatigue behavior is shown in Fig. 3a, where the maximum cyclic stress level, σ_{max} , is plotted versus the number of cycles to failure, N_f . The specimens loaded under the interrupted fatigue pattern sustained significantly more cycles than those loaded continuously until failure. The effect was more pronounced at high stress levels, with average lifetime increases reaching 126% at the level of 68 MPa, while being much moderate at lower stress levels, showing a 34% average increase at the level of 47 MPa. The applied fatigue loading patterns induced cyclic stresses in the linear region of the quasi-static stress strain curves derived by applying the same loading rate, as shown in Fig. 2. The strains reached at failure due to fatigue loading under either loading pattern increased with increasing stress level; however, they remained well below the quasi-static strains to failure, as shown in Fig. 3b. In addition, the failure strain was slightly greater when interrupted loading pattern was applied.

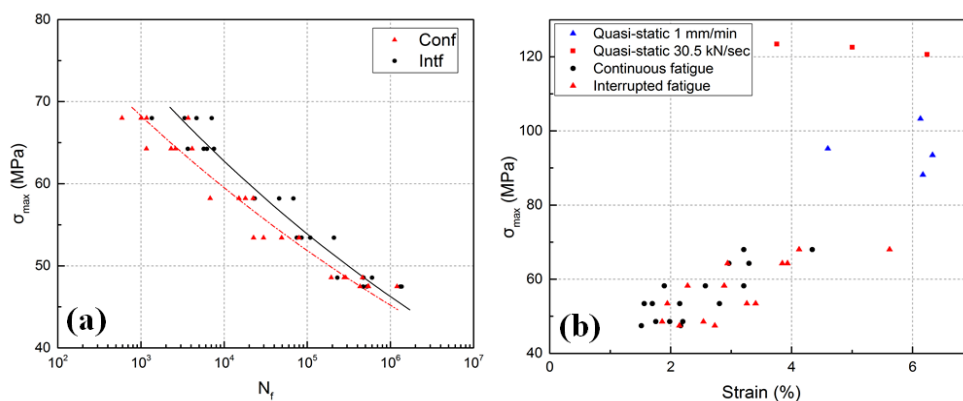


Figure 3. (a) Experimental fatigue data and S-N curves, (b) failure strain under different loading conditions.

The fatigue stiffness of specimens, defined as the slope of each hysteresis loop, loaded under continuous and interrupted loading at high and low stress levels is compared in Fig. 4a and b. A similar trend of stiffness degradation was observed at both stress levels as a result of damage formation and growth, i.e. an initial steep decrease during the first 10-15% of the lifetime followed by a steady state stiffness decrease up to specimen failure. At high stress levels, by applying interrupted loading, the stiffness at failure decreased considerably more than in specimens subjected to continuous loading. This confirmed that the former specimens accumulated much more damage than the latter ones until failure. The rate of stiffness degradation was, however, lower under interrupted loading. At low stress levels, the stiffness difference and thus the effect of interruption almost disappeared. The same comparison of the different loading patterns is shown for the evolution of the hysteresis loop areas in Fig. 5a for high and Fig. 5b for low stress levels. The hysteresis area (indicating energy dissipation) increased with the number of cycles at all stress levels. The values increased rapidly in the first loading block and then reached a steady state, which lasted for 80-90% of the fatigue life up to failure. Internal friction in damaged regions was the main cause of this energy dissipation [10]. At high stress levels, much larger hysteresis loop areas before failure were observed for the specimens under interrupted loading, again indicating far greater energy dissipation and thus damage accumulation. The rate of damage accumulation was however lower under interrupted fatigue loading. At low stress levels, the differences again almost disappeared.

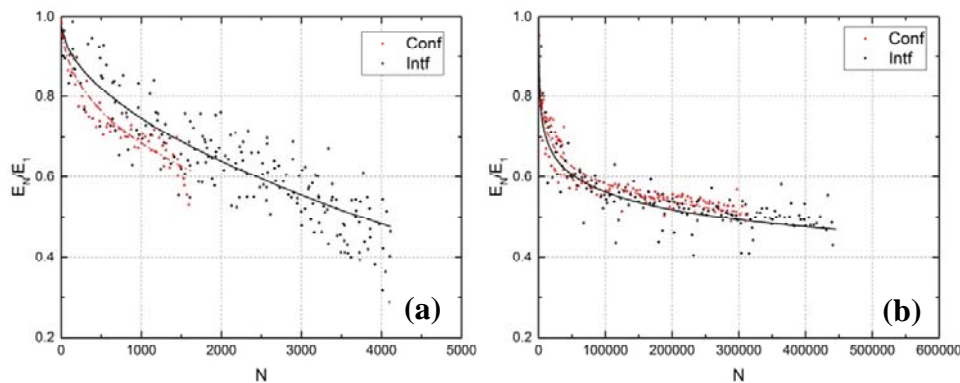


Figure 4. Average normalized fatigue stiffness versus number of cycles at $\sigma_{\max}=68$ MPa (a) and 49 MPa (b).

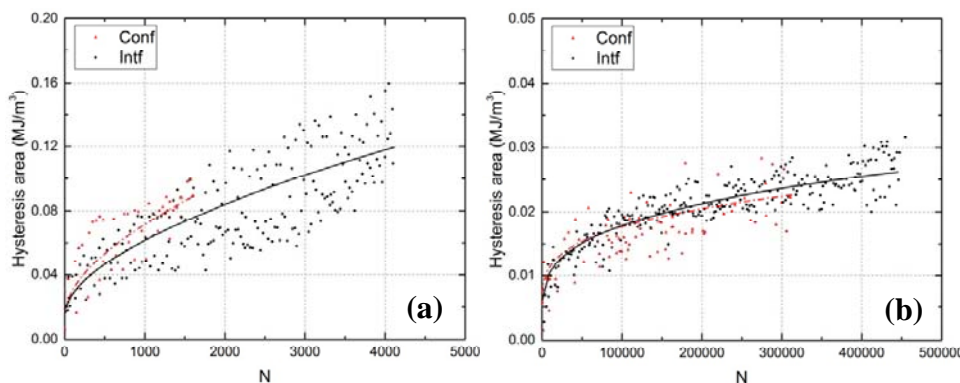


Figure 5. Average hysteresis area per cycle versus number of cycles at (a) $\sigma_{\max}=68$ MPa and (b) $\sigma_{\max}=49$ MPa.

Observation of Fig. 6a reveals that the fatigue stiffness was partially restored after each loading interruption; the restoring effect, however, decreased with decreasing stress level. This restoring of material stiffness was attributed to the recovery of the time-dependent stiffness component of the viscoelastic polymeric matrix. Similar to the stiffness, each curve of the hysteresis area in Fig. 6b was composed of small segments attributed to each loading block; they exhibited initial increase and then a steady-state stage. After interruption, the next segment started at a lower level, i.e. less energy was dissipated in the first cycle after interruption than in the last cycle before interruption. The mentioned material stiffening, which decreased the amount of internal friction and delayed damage formation due to increased fracture toughness, was the cause of the lower amount of dissipated energy at the

beginning of each loading block. With an increasing number of cycles, damage formation resumed and friction and therefore the hysteresis area increased.

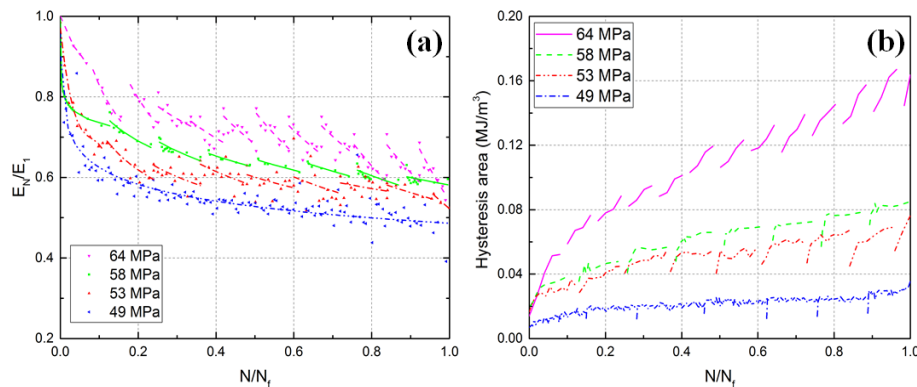


Figure 6. (a) Normalized fatigue stiffness and (b) hysteresis area per cycle versus normalized number of cycles.

As a result of the viscoelastic nature of the polymeric matrix, when the applied stress decreases, the material recovers and the specimen strain decreases with time. Fig. 7a shows, for three loading blocks, how the hysteresis loops were back-shifted on the strain axis from the last cycle after interruption to the first cycle of the subsequent reloading. The reduction of the average strain, $\Delta\varepsilon_{av}$, as a function of the stress level is shown in Fig. 7b. The strain reduction increased with the increasing number of cycles and fatigue stress level. It is seen that the increase of strain reduction with number of cycles was negligible at low stress levels; however, it gradually became considerable at higher stress levels.

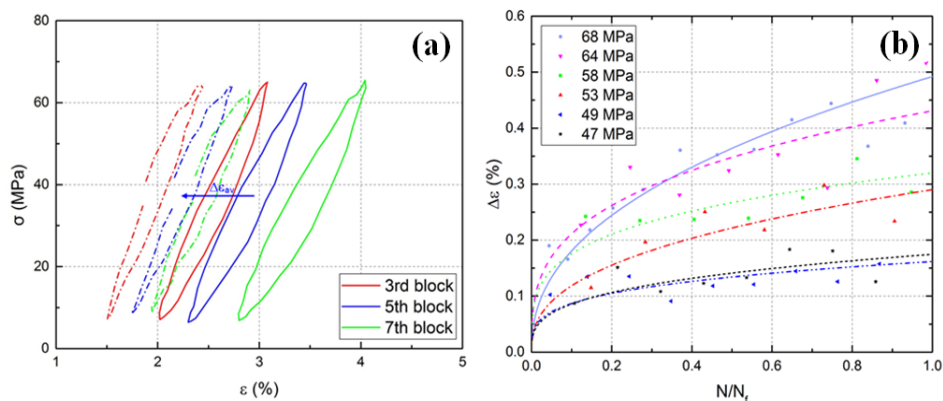


Figure 7.(a) back-shift of hysteresis loop (strain reduction) from last loop before interruption (solid line) to first loop (dashed line) of subsequent reloading, and (b) evolution of strain reduction versus normalized number of cycles at different stress levels.

Fig. 8a and Fig. 8b show the evolution of specimen transparency and the distribution of the self-generated temperature across the surface at different percentages of specimen fatigue life for the specimens, which loaded continuously and interruptedly at $\sigma_{max}=68$ MPa. The formation of any form of cracks in the matrix and fiber matrix debonding, mainly when the crack surface was perpendicular to the beam of light, caused light scattering and changed the specimen transparency. Therefore, darker regions in the photos correspond to decreased light transmittance due to greater damage formation. As shown for both cases, with an increasing number of cycles, damage gradually appeared along the fibers, at around 45° with respect to the specimen longitudinal axis, which was thus attributed to matrix/fiber interface debonding. Damage was more concentrated in the specimen loaded continuously while it was more evenly distributed throughout the specimen volume for interruptedly loaded specimen. This happened because, at low stress levels, the matrix and interface at the localized damage region were still able to transfer stresses to adjacent areas and the material had the ability to

develop and spread additional damage in the volume, and therefore dissipate more energy before failure. In all cases, failure with minor necking occurred in the region where significant damage was observed. In addition, it is seen that the different stress levels at both loading patterns led to different damage distributions. At higher stress levels the damage was severe and localized and caused the failure of these specimens at shorter lifetimes; however, by decreasing the fatigue stress level, more uniform and less severe damage distribution was observed throughout the specimen volume, which resulted in the longer fatigue life.

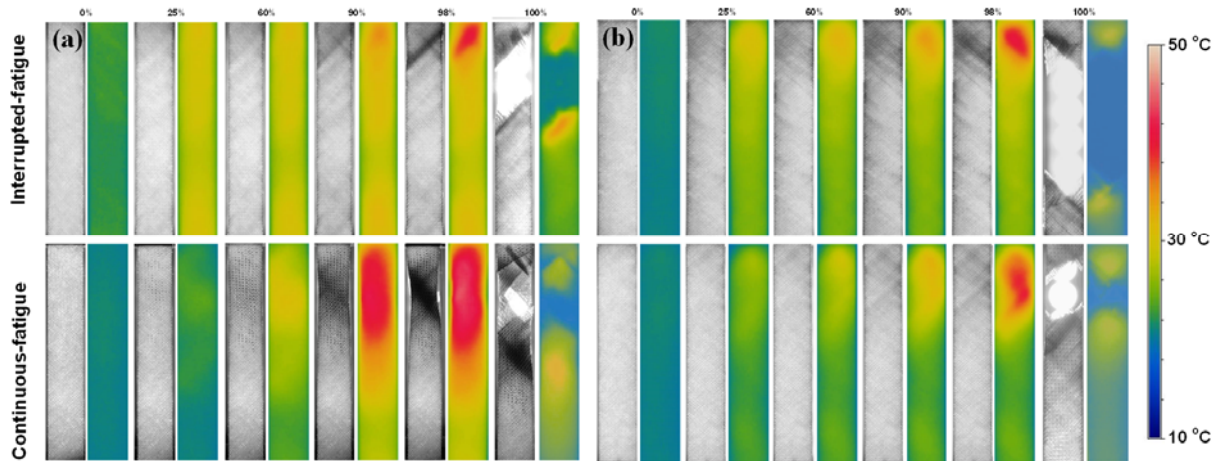


Figure 8. Pairwise representation of light transmittance and self-generated temperature for different percentages of fatigue life in interrupted and continuous fatigue loading patterns at (a) $\sigma_{\max} = 68$ MPa, and (b) $\sigma_{\max} = 47$ MPa.

The thermal camera revealed, during the early stages of the fatigue life, a uniform distribution of surface temperature, in both loading patterns. However, by increasing the number of cycles, the distribution of the temperature became more uneven, and hotspots, i.e. regions of high temperature concentrations, started appearing, which had an oval shape oriented in the fiber direction. These temperature increases were attributed to internal friction in damaged zones.

Comparison of the transparency and temperature distributions on the specimens' surfaces in Fig. 8a and Fig. 8b showed that damage was much more evenly distributed along the specimen under interrupted loading, while it was more concentrated, at the subsequent failure location, under continuous loading. This damage distribution throughout the whole specimen volume now explains why much more damage could be accumulated up to failure under interrupted loading. The effect of loading interruption on the damage distribution became negligible at low stress levels, while damage was evenly distributed throughout the specimen volume for both loading patterns. Two main mechanisms have been observed at the failure of all specimens; fiber breakage and fiber pull out. The fatigue fracture surfaces of representative specimens examined at different stress levels are shown in Fig. 9. For all cases, a diagonal damage pattern, following the 45° fiber direction, was observed. For higher stress levels, Fig. 9a and b, the failure was characterized by extensive fiber pull-out, a consequence of the significant deterioration of the matrix/fiber interfaces, which hindered the transfer of the stresses from the matrix to the fibers at the concentrated damage zones. The failure modes did not exhibit any significant differences by applying different loading patterns, while only the necking was more pronounced under continuous fatigue loading. By decreasing the fatigue stress level, a mixed-mode failure with fiber pull-out and fiber breakage was observed with predominant fiber breakage at the lowest stress level, as shown in Figs. 9c and d. The presence of fiber breakage at low stress levels was attributed to the more uniform and less severe damage distribution, which allowed the matrix and interface to transfer stresses to the fibers.

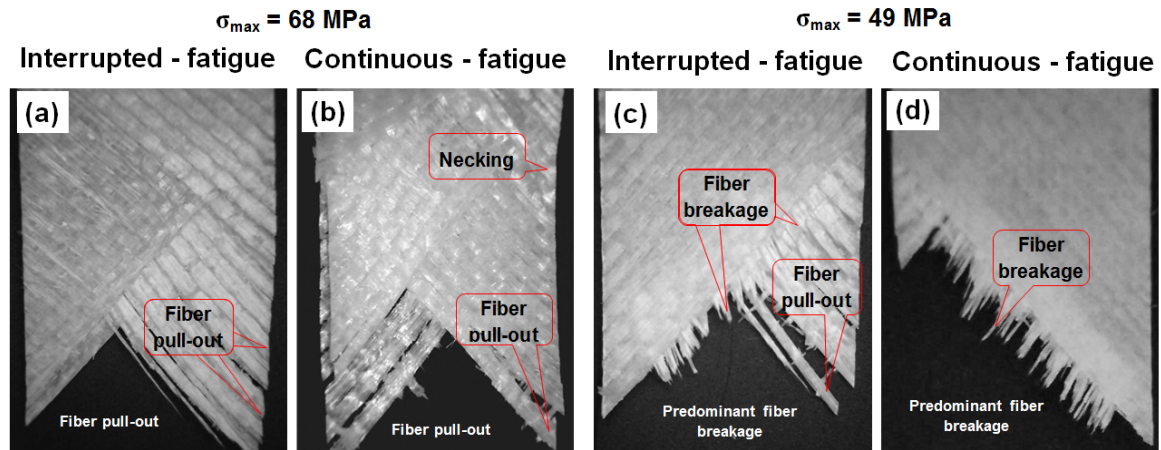


Figure 9. Fatigue fracture surfaces under different loading patterns and stress levels.

3.3. Damage retardation and distribution mechanisms

The enhancement of fatigue life in the specimens loaded under interrupted fatigue loading was attributed to basically two crack-growth retardation mechanisms, which retarded or even arrested crack growth and led to the observed better damage distribution and thus longer fatigue life. Both mechanisms were based on the viscoelastic nature of the matrix. In the first mechanism, the repeated material stiffening at the beginning of each loading block with respect to the previous loading block increased the material fracture toughness, which temporarily retarded the crack growth. Material stiffening increased with increasing stress level, which thus caused more crack growth delay at higher stress levels. This mechanism explained the general damage formation delay under interrupted fatigue loading, but not the better distribution across the specimen volume caused by the latter. In the second mechanism, unloading the damaged viscoelastic matrix led to crack blunting, i.e. the local stress intensity in the craze zone at the crack tip was significantly reduced and did not increase again at the same rate as the reloading and thus delayed the crack growth in the following cycles [11]. This delay further enabled the initiation and growth of new cracks at other locations and thus led to the observed distribution of damage throughout the whole specimen volume. Crack blunting and the resulting damage growth delay and better distribution of damage increased with increasing stress level [11]. In addition, the interruptions also decreased the self-generated temperature compared to the continuous loading and thus reduced potential material softening, which would have affected the fatigue life.

3. Conclusions

The tensile-tensile interrupted fatigue behavior of angle-ply, $(\pm 45)_{2s}$, glass/epoxy composite laminates has been experimentally investigated in this work. Different mechanical, thermal, and optical measurements were performed for the study of the specimens' fatigue behavior at different stress levels. The experimental results were compared to those obtained by continuously loading the same type of specimens until failure. The following conclusions were drawn:

- The specimens loaded under interrupted fatigue had longer fatigue lives than those continuously loaded at the same cyclic stress levels. The enhancement of fatigue life was attributed to the delayed crack growth via the occurrence of crack blunting and material stiffening at the beginning of each loading block and also the specimen cooled down, which reduced potential material softening. The enhancement of fatigue life increased at higher stress levels.
- At high stress levels, under both loading patterns, failure was observed in the form of fiber pull-out; however, in specimens loaded continuously failure occurred with considerable

necking. At low stress levels, failure with predominant fiber breakage under both loading patterns was observed

- The fatigue stiffness was partially restored after each loading interruption due to the recovery of the time-dependent stiffness component of the viscoelastic polymeric matrix. The material stiffening and associated increase of fracture toughness also decreased the amount of energy dissipation at the beginning of each loading block. These effects of interruption were dependent on the stress level and almost disappeared at low levels.
- By applying an interrupted fatigue loading pattern, the rate of stiffness degradation and energy dissipation per cycle decreased due to the delayed damage growth. In addition, more uniform damage growth throughout the specimen increased the specimen's capacity to accumulate damage, which led to lower stiffness at failure, greater energy dissipation per cycle at failure.

ACKNOWLEDGMENTS

The authors wish to acknowledge the support and funding of this research by the Swiss National Science Foundation (Grant No. 200021_156647/1).

References

- [1] K. L. Reifsnider, and A. Talug. Analysis of fatigue damage in composite laminates. *International Journal of Fatigue*, 2.1:3-11, 1980.
- [2] A. Varvani-Farahani, H. Haftchenari, and M. Panbechi. An energy-based fatigue damage parameter for off-axis unidirectional FRP composites. *Composite Structures*, 79.3:381-389, 2007.
- [3] B. Vieille, and W. Albouy. Fatigue damage accumulation in notched woven-ply thermoplastic and thermoset laminates at high-temperature: influence of matrix ductility and fatigue life prediction. *International Journal of Fatigue*, 80:1-9, 2015.
- [4] A.P. Vassilopoulos, and T. Keller. *Fatigue of fiber-reinforced composites*. Springer Science & Business Media, 2011.
- [5] L.J. Broutman, S.K. Gaggar. Fatigue behavior of epoxy and polyester resins. *International Journal of Polymeric Materials*, 1.4:295-316, 1972.
- [6] W.A. Herman, R.W. Hertzberg, J.A. Manson. The influence of loading history on fatigue in engineering plastics. *Journal of Materials Science*, 25.1:434-440, 1990.
- [7] A. Gagel, D. Lange, K. Schulte. On the relation between crack densities, stiffness degradation, and surface temperature distribution of tensile fatigue loaded glass-fibre non-crimp-fabric reinforced epoxy, *Composites: Part A*, 37:222–228, 2006.
- [8] A.V. Movahedi-Rad, T. Keller, A.P. Vassilopoulos. Fatigue damage in angle-ply GFRP laminates under tension-tension fatigue. *International journal of fatigue*, 109:60-69, 2018.
- [9] A.V. Movahedi-Rad, T. Keller, A.P. Vassilopoulos. Interrupted tension-tension fatigue behavior of angle-ply GFRP composite laminates. *International journal of fatigue*, 113:377–388, 2018.
- [10] R. Chandra, S.P. Singh, K. Gupta. Damping studies in fiber-reinforced composites—a review. *Composite structures*, 46.1:41-51, 1999.
- [11] R.A. Schapery. A theory of crack initiation and growth in viscoelastic media. *International Journal of Fracture*, 11.1:141-159, 1975.